Hindawi
International Journal of Chemical Engineering
Volume 2023, Article ID 7302409, 9 pages
https://doi.org/10.1155/2023/7302409

Research Article

Synthesis of Micromesoporous Zeolite-Alumina Catalysts for Olefin Production from Heavy Crude Oil

M. Al-Samhan, J. Al-Fadhli, A. M. Al-Otaibi, and R. Bouresli

Petroleum Research Centre, Kuwait Institute for Scientific Research, P.O. Box 24885, Safat 13109, Kuwait

Correspondence should be addressed to M. Al-Samhan; msamhan@kisr.edu.kw

Received 20 December 2022; Revised 19 January 2023; Accepted 23 January 2023; Published 31 January 2023

Academic Editor: Pedro Castano

Maximizing the production of high-value olefins from heavy crude oil is a crucial topic in the downstream refining industry. However, converting heavier fractions is a major challenge due to the small pore size of the zeolites. Therefore, this work aimed to develop extrudate zeolite catalysts posing adequate micromesoporous pore network and moderate acidity by combining microporous zeolite with the boehmite phase of alumina. These extruded zeolite-alumina catalysts are expected to allow sufficient diffusion of heavy fractions, thus leading to high cracking of heavy oil into valuable olefins. Different zeolite-alumina catalysts of varying alumina content ranging from 25 to 75% (AlZ-25, AlZ-50, and AlZ-75) were prepared in the laboratory to study the optimum zeolite-alumina ratios for maximum olefin production from heavy oil. The catalysts were characterized for their chemical and physical properties using nitrogen adsorption (N_2 adsorption), X-ray diffraction (XRD), inductively coupled plasma (ICP) spectrometry, Fourier transform infrared (FT-IR) spectroscopy, and NH_3 temperature programmed desorption (TPD). A gradual increase in the average pore diameter (APD) of the catalysts was observed due to the alumina ratio with a distinct range of acidity that is in the range of 125 to 375°C, and also the geometry of pores is not the same for all of the supports. Catalytic performance tests were conducted in a fixed-bed reactor at 450°C, 10 bar, and liquid hourly space velocity (LHSV) of 1 h^{-1}. The results revealed that the prepared catalysts were thermally stable and effective in heavy oil conversion to olefins. Moreover, the selectivity of propylene was higher than that of ethylene (P/E) due to the modified textural and acidic properties of the catalysts. The results showed that the catalysts prepared with moderate acidity and adequate mesopores exhibited a considerable effect on the conversion of heavy crude oil into olefins. Hence, the acidity and mesoporosity of the catalysts play a vital role in determining the catalyst performance.

1. Introduction

The world's demand and production of olefins are now higher than any other chemicals. Olefins are common raw materials for plastics' production, fibers, and other chemicals that are converted into daily goods ranging from computer parts to pharmaceuticals [1]. The strategy for most of the new refineries is based on the need for maximizing the economy, by expanding the utilization of natural resources (such as heavy oil) for light chemicals and petrochemical industries [2]. However, the main constraint for this needed expansion is the inexpensive processes of the feedstock [3]. Currently, crude oil-to-chemicals (COTC) is a powerful industry driver and a strong trend of high interest to all integrated refineries and chemical producers [4, 5]. This is reinforced by a number of factors, most notably with the forecast predicting a slowing down of transportation fuel growth approaching 2040, timed with the growth in chemicals (e.g., olefins and aromatics) [6]. Heavy crude oil and residual oil cracking processes for the production of olefins are currently semicommercial, which is mainly due to the lack of catalyst stability and a method of preventing coking trouble in the reactor [7–9]. Hakimian et al. reported HZSM-5 for producing high chemicals from oil sludge [10]. Cheng and Huber studied HZSM-5 for furan conversion into aromatics and olefins [11].

Therefore, the catalyst selection for such a process is grounded on coke resistant, a complex association of particle size, activity, and pore size grading [12, 13]. A zeolite-based catalyst is a major cracking catalyst used in the industry

[14, 15]. The sodium–Y zeolite support composition can be optimized with the combination of alumina, which will dilute zeolite acid sites and contribute to the larger pores. The accessibility of zeolite pores becomes crucial in heavy crude or residue feedstock; thus, the larger pore may enhance feed diffusion and enhance stability toward deactivation [16, 17]. Numerous research institutes and oil companies are studying the foretasted direct cracking processes and trying to overcome the related drawbacks of each process in order to reach a cost-effective production [18, 19]. Synthetic zeolites can be designed to selectively perform specific tasks, and with a typically more homogeneous composition than the case for their naturally occurring counterparts. A superlative example of a tailored synthetic zeolite is H-ZSM-5, developed by Mobil in the early 1970s [20]. The combination of cation-exchange and microporous capacity confers particular properties to zeolites and a wealth of applications for them. Nazi Rahimi and Ramin Karimzadeh reported in their review on the influence of different factors, such as the ZSM-5 acidity, Si/Al ratio, and the temperature, on light olefin production [21, 22].

Others reported that for olefin production to obtain mesoporous ZSM-5 zeolites in which the integrity of the essential structure is preserved [23, 24], the simplest way is to remove percentage of silica from a zeolite by treatment with alkaline solutions. The process is optimal at a range of Si/Al ratios of 25–50 while at higher Si/Al ratios, the loss of framework silicon becomes excessive and unselective, at lower ratios, comparatively little extraction of silicon occurs.

The accessibility of the zeolite pore becomes crucial in heavy crude or residue feedstock; thus, the larger pore may enhance feed diffusion and enhance stability toward deactivation [25, 26]. Numerous research institutes and oil companies are studying the afforested direct cracking processes and trying to overcome each process-related drawback to reach a highly cost-effective production [27, 28].

In this work, three prototype catalysts were prepared with an in-depth understanding of the behavior of heavy oil under high temperature toward direct production of olefin. The novelty in this work includes direct cracking of heavy oil using an extrudate shape catalyst in a bed reactor. The Y-zeolite catalyst was selected based on the suitability for direct cracking and altering the pore size to fit heavy molecules. The methodology in this study includes the preparation of different composition of Y-zeolite in alumina (i.e., 25%, 50%, and 75%wt) then characterized for their physical and chemical properties. Then, tested for optimum yield and product quality under different operating conditions using readily equipped pilot plants and fixed-bed reactors.

2. Materials and Experimental Work

Prototype catalysts: The three types of catalysts were prepared with different silica alumina ratios. All samples were subjected for physical and chemical characterization using the following techniques:

2.1. Catalyst Preparation. This study focuses mainly on the preparation of zeolite-alumina catalyst posing large pore size and moderate acid-base properties, which are conducive for heavy oil conversion into olefins. The zeolite-alumina catalysts (300 g) were prepared by mixing the Y-zeolite (CBV 300; Si/Al = 2.55), boehmite alumina (Versal), and polyethylene glycol (PEG 4000). The amount of boehmite alumina in the catalyst has varied from 25 to 100% which resulted in four catalysts, namely, Al-Z-25, Al-Z-50, Al-Z-75, and Al-100, respectively. The boehmite alumina, PEG, and Y-zeolite mixture was first physically mixed, and then the mixture was peptized using 2.5 vol% nitric acid (170 mL) as a peptizing agent [29]. The volume of the peptizing agent varied slightly depending upon the support composition (i.e., boehmite alumina/Y-zeolite ratio). The obtained dough was extruded in a mechanical extruder. These extrudates were dried, and then calcined before subjected to characterization. The composition of the prepared catalysts and their textural properties are reported in Table 1, whereas the flow scheme of the catalyst preparation is provided as Figure 1.

2.2. Catalyst Characterization. The surface morphology and elemental analysis of the catalyst extrudate were studied using a scanning electron microscope (JEOL-JSM-IT300) coupled with energy dispersive X-ray (EDX). The NH_3-TPD was undertaken to study the strength of the acidic sites and desorbed species on the catalyst surface by using a Qunatachrome instrument. For NH_3-TPD analysis, the sample was loaded into a quartz microreactor, pretreated at 700°C in helium (He) gas and then subjected to NH_3 atmosphere. The FTIR spectrum was composed of 64 scans (spectral resolution of 4 cm^{-1}). Details of characterization equipment and methods are described as follows:

(i) *Textural Properties of Support/Catalysts*. Mercury porosimetry is used as a characterization technique to provide a wide range of information such as pore volume, pore size distribution, pore diameter, and the specific surface area. The catalyst materials were also determined by the Brunauer–Emmett–Teller (BET) method. An ASAP 2020 surface area analyzer manufactured by the Micromeritics Corporation was used for the BET adsorption isotherm and surface area determinations at 77K.

(ii) *Temperature Programmed Desorption*. The TPD experiment is carried out using ammonia gas. The gas is initially adsorbed on the catalyst support surface, and then the surface is heated at a controlled rate (programmed rate), which causes the adsorbates to react and desorb from the surface. A TCD detector is used to monitor the desorption products. As the catalyst is saturated with the adsorbed NH_3, helium is used for flushing the physically adsorbed NH_3 until the baseline is stable. The NH_3-TPD was then carried out in a constant flow of He (20 ml/min) from 150°C to 700°C at a heating rate of 10°C/min. The concentration of

Table 1: Properties of prepared catalyst support.

Sample ID	Support composition	BET			Porosimetry		
		SSA (m^2/g)	TPV (cc/g)	APD (Å)	TPV (cc/g)	PA (m^2/g)	APD (Å)
Al-100	Versal alumina (100%)	274.8	0.691	66	0.638	266.9	96
Al-Z-25	CBV-300 (25%) + versal alumina (75%)	340.8	0.596	76	0.742	207.4	143
Al-Z-50	CBV-300 (50%) + versal alumina (50%)	425.6	0.411	72	0.702	132.7	211
Al-Z-75	CBV-300 (75%) + versal alumina (25%)	559.2	0.282	57	0.749	69.6	431

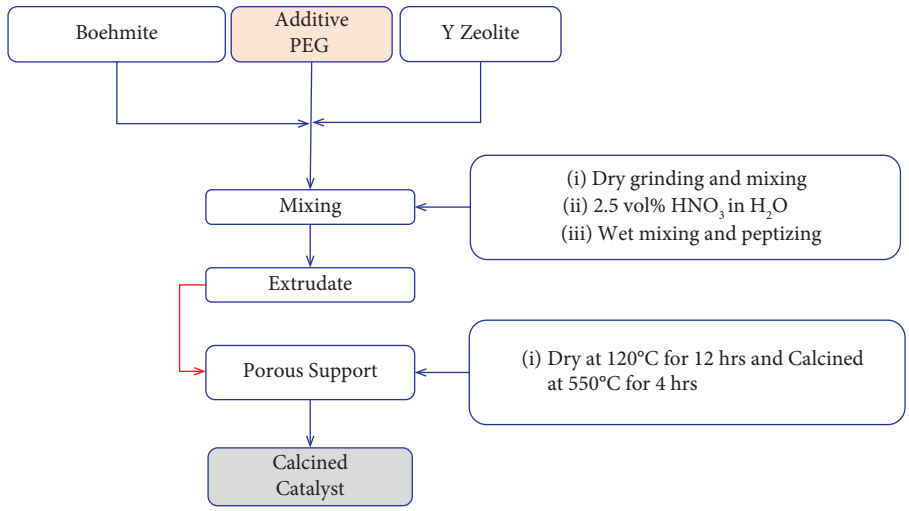

Figure 1: Flow diagram of the catalyst preparation and its treatment conditions.

ammonia (NH_3) in the exit gas was monitored continuously using a gas chromatograph equipped with a TCD.

(iii) *Fourier Transform Infrared Spectroscopy (FT-IR).* FTIR is a surface analysis technique that was used to identify the functional groups in the spent catalysts. The main objective of this characterization is to ascertain the nature of coke species. The surface-deposited (foreign species) and active metals species were confirmed with the Fourier transform infrared spectroscopy (FT-IR) analysis, Vertex 70/80, type 127000, manufactured by Bruke.

2.3. Catalyst Performance Evaluation. Catalytic performance tests were conducted in a pilot plant fixed-bed reactor at 450°C, 10 bar, and liquid hourly space velocity (LHSV) of $1\ h^{-1}$. The experiments were conducted for 48 h. During the experimental run, the samples were collected to analyze them for olefin content using the bromine number.

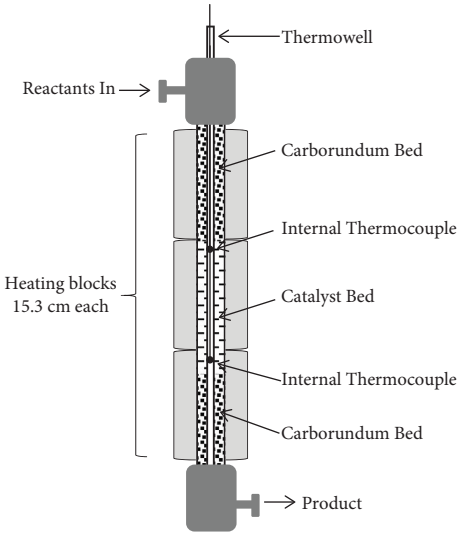

Figure 2: Schematic illustration of the reactor and catalyst loading.

2.3.1. Flow Reactor Catalytic Activity Testing. A continuous flow pilot plant consists of one fixed-bed isothermal reactor was used for testing, as shown in Figure 2. The pilot plant is equipped with a metered gas flow system, metered liquid flow system, gas/liquid separation system, liquid product collection system, and product gas metering system. The pilot plant is fully automated, and it is controlled by a stand-alone advanced control system designed and built by Allen Bradley for advanced control systems. The reactor is a hollow cylinder of 0.7 centimeters (cm) in diameter and 46.0 centimeters in length. During testing, heat is supplied to the reactor through three independent electrical heating blocks housed in one shell. Each heating block is equipped with two thermocouples: one is used to control the reactor's external surface temperature and the other one is used to shut down the heating block in case of temperature runaway. Internal temperature is measured by two internal thermocouples housed in a thermowell of 0.3 centimeters in

diameter, which extends to top to bottom of the central axis of the reactor's cavity. Figure 2 shows a schematic diagram of the reactor.

2.3.2. Heavy Crude. The feed that was used in this study was the heavy crude oil collected from Kuwait Oil Company (KOC). This crude oil is produced from the northern oil fields of Kuwait, and it is classified as heavy crude oil. The heavy crude oil was filtered and dewatered, followed by desalting step at the Petroleum Research Centre (PRC), before it was introduced to the reactor for testing. Table 2 presents the key properties of the heavy crude oil.

2.3.3. Online Gas Analysis. A gas chromatography (GC) apparatus was used to establish an online analysis of the gas product during testing. The single channel GC was connected to the pilot plant and the batch reactor gas outlet systems through a network of tubes. A DB-PETRO 100 m long, 0.25 mm inner diameter, and 0.50 μm film thickness column was installed and few injections with standard mixture gases were injected to evaluate its suitability for analysis and conditions for the desired ethylene and propylene. The standard gas mixture is composed of saturates, olefins, and isomers. After calibration, the GC operating conditions were optimized to precisely identify the functional peaks of the methane, ethane, ethylene, propane, propylene, and its derivatives.

3. Results and Discussion

3.1. Textural Properties. Specific surface area (SSA), total pore volume (TPV), average pore diameter (APD), and pore area (PA) were measured to determine the suitability of the prepared catalyst for olefin production and selectivity. The composition of catalysts and their properties is shown in Table 1 using the Brunauer–Emmett–Teller (BET) method. The N_2 adsorption isotherm at 77K, that is, relative pressure p/p 0 versus adsorbed volume in cc^3/gram of catalyst is shown in Figure 3.

As can be seen from the results (Figure 3(a)), the pure zeolite-Y followed type 1 isotherm [30]. N_2 uptake was relatively higher in the Y-zeolite at a lower pressure region (P/P_0 = 0.04) followed by AlZ-50 and Al100. The pore size distribution (Figure 3(b)) also indicated the microporosity in the Y-zeolite. In contrast, the zeolite-alumina catalysts followed type IV isotherms with a clear hysteresis loop, which indicates that these catalysts pose mesoporous structure. The APD of all the samples (57–76 Å) also confirmed the mesoporosity of the samples. The mesoporosity in the catalysts was introduced due to the addition of boehmite alumina which poses a wide pore size distribution. The pore size distribution also indicated the microporous and mesoporous distribution of the catalyst samples. Also, as the concentration of alumina increases, a gradual increase in the APD of the catalyst was observed which further confirmed that alumina contributed to the mesopores. In the case of the BET surface area, the highest SSA was observed for the sample (Al-Z-75) having maximum Y-zeolite concentration (75%), whereas the lowest SSA was observed for the sample (Al-100) posing Y-zeolite contribution.

The catalysts contain large pores and pore size distributions for heavy oil processing, measured by mercury (Hg) porosimetry. The textural properties of catalysts are characterized using Hg intrusion-extrusion, whose data are used to derive the total pore volume and pore size distribution, as shown in Figure 4. The support contains a bimodal type of pore-size distributions derived from the intrusion data which are presented in Figure 5 inset.

Various supports were prepared, which have moderate SSA in nature and contain a total pore volume in the range of 0.2 to 0.7 ml/g. However, the exact shape of the pore diameter varies from one catalyst to another, which indicates that the geometry of pores is not the same for all of the supports, as shown in Figure 6. The main purpose of measuring texture by two techniques is that the BET method can effectively measure only micropores while Hg porosimeter can measure mesopore and macropore. The prototype catalyst contains both the microporous and macroporous, which are generated due to zeolite and alumina combination and combined contribution, respectively.

3.2. Temperature Programmed Desorption (TPD). The number of acid sites was measured by using NH_3-TPD, which monitor the desorbed ammonia. The number of acid sites (weak, medium, and strong) present in the catalysts is shown in Figure 7. The desorption peak area represents the amount of acid sites, and the peak temperature represents the acid strength. The peak below at 125°C was related to the weak acid sites, while the peak higher than 375°C represents the strong acid sites. The peaks between 225 and 375°C are related to medium strength acid sites [31, 32]. It could be seen that the acidity of the prototype catalyst exhibited a distinct range of acidity that is in the range of 125 to 375°C. The results clearly suggest that catalyst having relatively higher Y-zeolite concentration exhibited higher peak intensity due to the presence of greater acid sites. A significant amount of Lewis sites is also available particularly where large amount of alumina (Lewis acid sites are mainly by extra-framework aluminum) is used as a binder. Lewis sites may have a potential effect on increasing nearby Brönsted acid sites and form the first carbonium ion in the cracking of alkanes.

3.3. FT-IR. The FT-IR studied the qualitative comparisons of the various functional groups present in the catalysts. The zeolite framework spectra of samples can be observed with the 950 cm^{-1} peak in association with the binder (alumina). The specified 950 cm^{-1} peak is the zeolite framework nature of the Si-O-Al structure [33], which moves with increasing alumina concentration in the catalyst, as shown in Figure 8(a). For comparison, Figure 8(b) shows an infrared spectrum of alkaline earth metal (Mg) and rare Earth (La) metals over the base catalyst AlZ-50. The number of different functional groups and structural hydroxyl groups was observed for catalysts containing alkali cation. The frequency of

Table 2: Crude oil properties and feedstock preparation.

Property	Unit	Fresh crude oil	After filter	*Final crude oil
Water content	wt%	2.00	1.90	1.90
Salt content	PTB	>150	>150	15.4
API		11.57	11.55	11.35
Specific gravity		0.989	0.989	0.991
Density				
@ 15°C	gm/cc	0.988	0.988	1.000
@ 65°C	gm/cc	0.957	0.957	0.958
Asphaltene	wt%	4.94	5.41	6.37
MCR	wt%	11.90	11.74	12.40
Sulfur content	wt%	5.27	5.23	4.84
Kinematic viscosity @ 40°	mm^2/s	783	789	928

• Final crude oil is desalted.

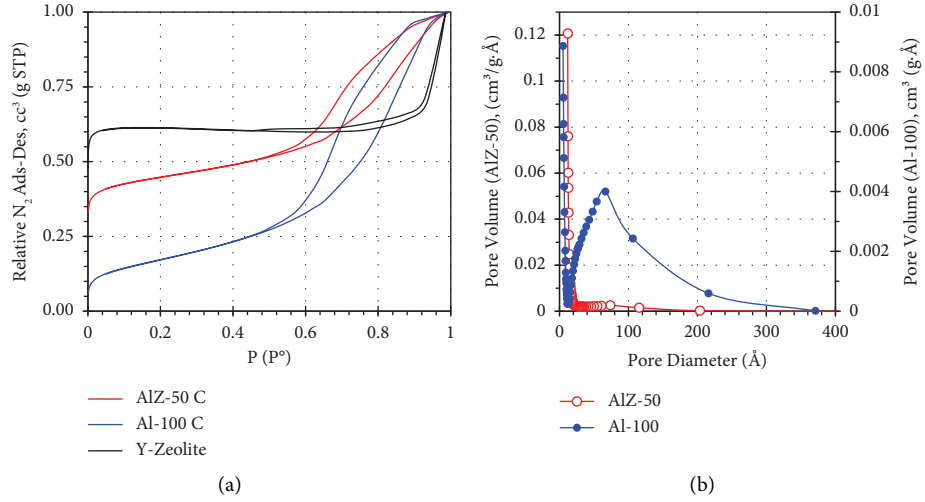

Figure 3: N_2adsorption-desorption isotherm and pore distribution.

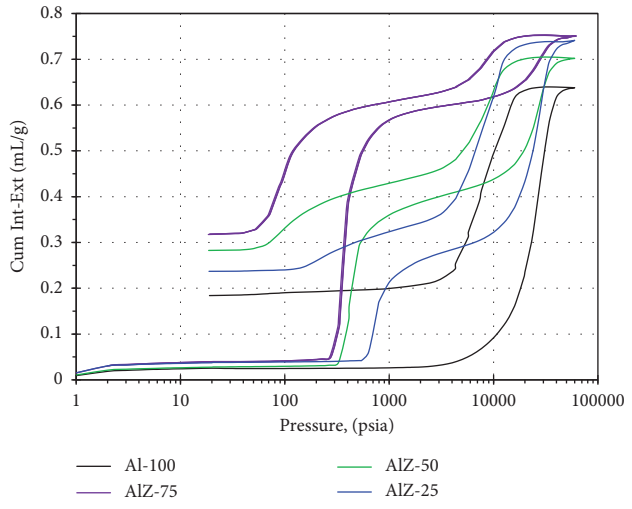

Figure 4: Hg intrusion-extrusion pressure and isotherms.

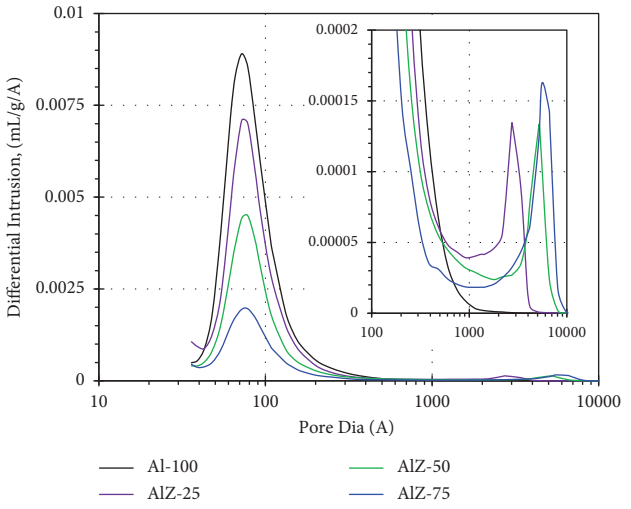

Figure 5: Variation of pore size distribution as a function pore diameter.

the absorption bands of the adsorbed water varied with the cation radius. The adsorption of water on the alkali cation zeolites is highly reversible. The spectra of magnesium and lanthanum Y-zeolites dominated with the structural hydroxyl groups. The absorption band 3600–3560 cm^{-1} region is identified with hydroxyl groups associated with the divalent cations, while a band near 3690 cm^{-1} is due to

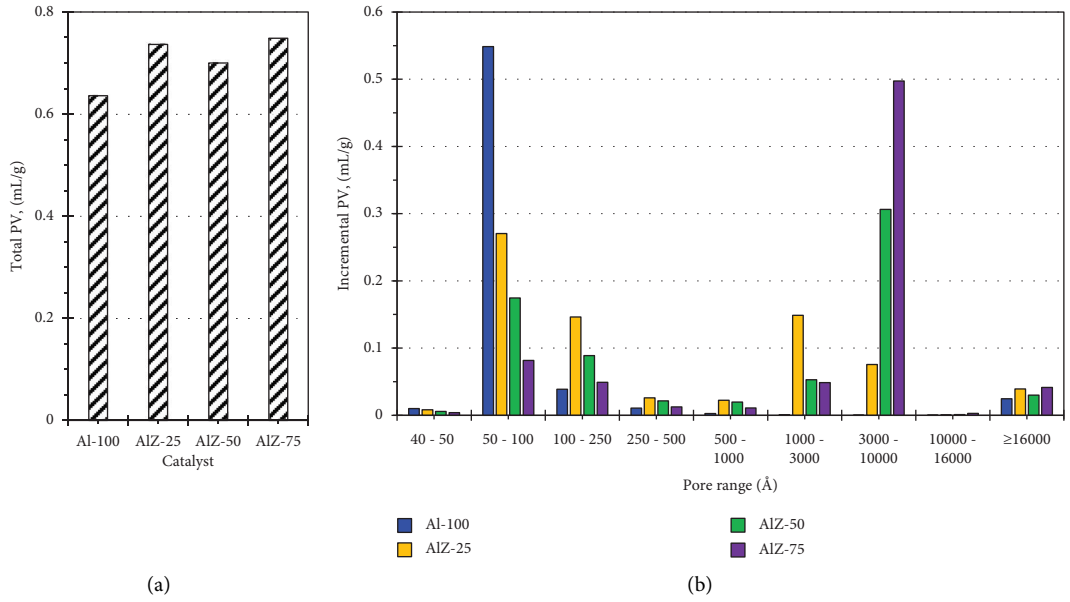

Figure 6: Variation of the total pore volume as a function of (a) catalyst composition and (b) range of pore size distribution.

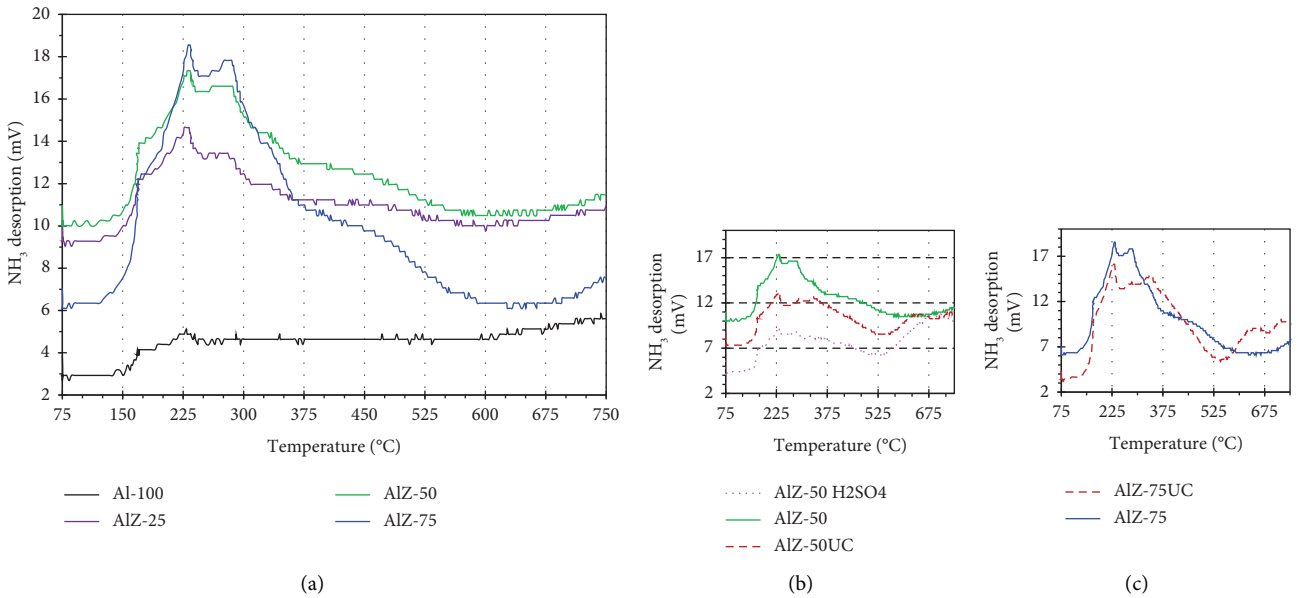

Figure 7: TPD spectra of the various amounts of zeolites (25, 50, and 75 wt% Y) containing catalyst.

adsorbed undissociated water. The typical nature of Y-zeolites has been observed (XRD) and which were also confirmed during TGA dehydration.

From the conducted tests, AlZ-50 was selected as optimum based on its acidity, thermal stability, and available pore in the catalyst. Therefore, further flow reactor studies were carried out using the AlZ-50 catalyst.

3.4. Cracking Activity and Fixed-Bed Reactor Evaluation. The selected prototype catalyst (ALZ 50) was tested using the fixed-bed reactor to evaluate the performance of the alumina and zeolite ratios. This part of the study required significant changes in the unit to connect the GC for online gas analysis calibrated mainly for C2 and C3. The gas analysis results were used to identify catalytic and operating conditions' functions, which are seen in Figure 9, the ratio of propylene to ethylene (P/E) is constant with time on stream (TOS) regardless of the difference in the temperature levels, which provide strong evidence that the catalyst performance was stable, and the P/E ratio was governed by thermodynamic limitations. On the other hand, it is clear that the temperature played a significant role on both compounds' conversion levels. In Figure 9(a), at 395°C, in average, the conversion is 0.45% for ethylene and 0.65% for propylene, but in Figure 9(b), at 400°C, conversion of both compounds from the feed (heavy crude) is observed to be 1.5 folds higher for ethylene and almost the double for propylene. In general,

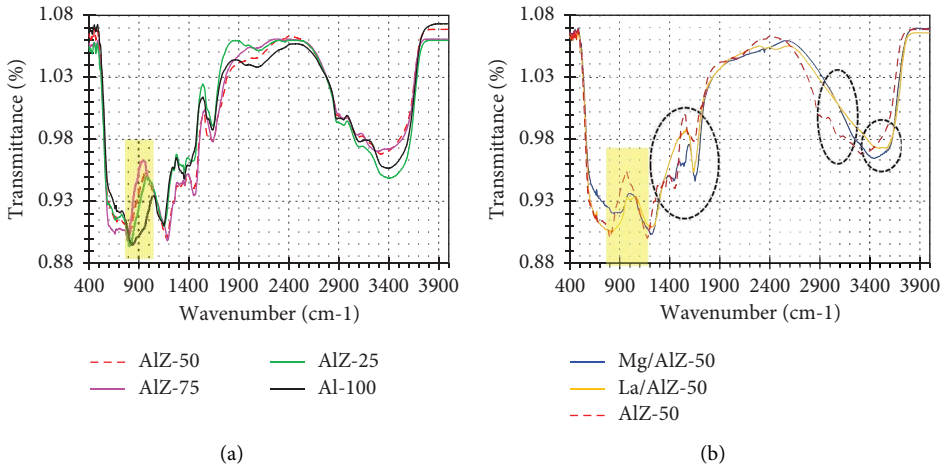

Figure 8: Oxide catalysts' surface functional group and structural parameters.

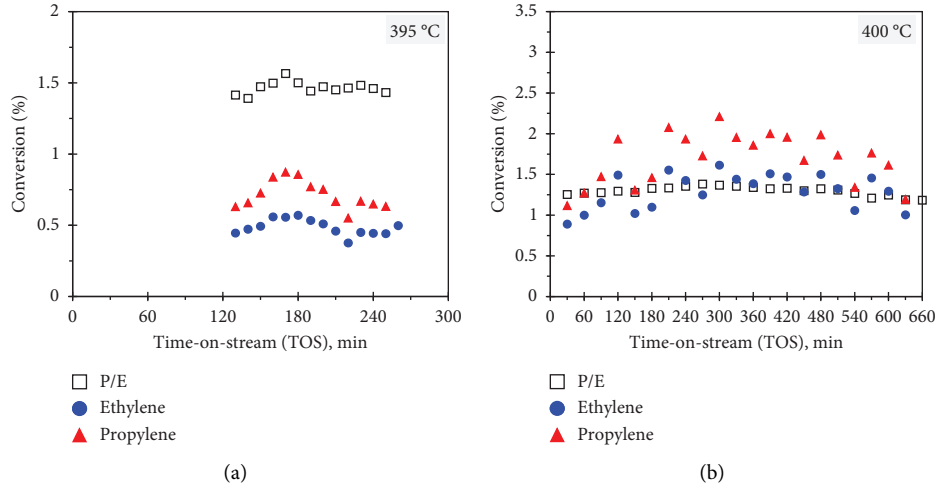

Figure 9: Catalyst performance at two temperatures with time on stream (TOS): LHSV = 1 h^{-1}; N_2/oil ratio = 250 mL/mL.

chemical reactions that are thermodynamically controlled (governed) are sensitive to temperature levels. Temperature can easily shift the thermodynamic balance between two compounds to favor one on the other. At 395°C, the P/E ratio was near 1.5, and at 400°C, the ratio dropped to 1.25 (almost 17% drop), while this drop can be attributed directly to the dramatic increase in ethylene conversion, the results lead to deduce that the catalyst selectivity is apparently sensitive to the increase in temperature, even a slight increase of 5°C, and the catalyst nature favors ethylene upon propylene with an increase in temperature, however within the allowable thermodynamic boundaries.

4. Conclusion

Three different alumina/silica ratios of the prototype zeolite catalysts were prepared and characterized for heavy crude conversion. AlZ-50 was selected as optimum based on its acidity, thermal stability, and pores in the catalyst. Textural results obtained from N_2 adsorption and mercury porosimeter have proven that the same characteristics measured by different techniques are not comparable because the characteristics measured by different techniques have different significance. A balance between support textural properties, acid-base properties, and the active composition variation was investigated for heavy oil conversion to the olefin formation. The integration between the pores and connectivity played an important role to balance between activity and selectivity particularly for the possible secondary reaction or dehydrogenation of the cracked molecules. The feed holdup within the catalyst has significantly lowered time in the case of fixed-bed reactors, in which textural properties play a critical role to diffuse reactants and product molecules within the extradite (i.e., inter- or intra-crystal particles).

The method of heavy oil conversion into olefin by using flow reactor systems was established, and reliable results were obtained during the catalytic processing. Based on the conversion, the significant work remains in the area of catalyst development, particularly acid-base function

synergy with the textural properties. An optimum balance between characteristic properties significantly contributed to the propylene to ethylene ratio, which is an indirect measure for the stability of the catalyst. Hence, future long-term client funded projects are expected in order to foresee heavy oil conversion value-added clean products in the future. It can be concluded that more petrochemical projects will be integrated with the existing work to ensure long-term competitiveness and sustainable business.

Data Availability

The data that support the findings of this study are available from the corresponding author upon reasonable request.

Conflicts of Interest

The authors declare that they have no conflicts of interest.

References

[1] E. Cetinkaya, N. Liu, T. J. Simons, and J. Wallach, *Petrochemicals 2030: Reinventing the Way to Win in a Changing Industry*, McKinsey on Chemicals, Atlanta, GA, USA, 2018.

[2] A. Corma, E. Corresa, Y. Mathieu et al., "Crude oil to chemicals: light olefins from crude oil," *Catalysis Science and Technology*, vol. 7, pp. 12–46, 2017.

[3] A. Corma, L. Sauvanaud, Y. Mathieu, S. Al-Bogami, A. Bourane, and M. Al-Ghrami, "Direct crude oil cracking for producing chemicals: thermal cracking modeling," *Fuel*, vol. 211, pp. 726–736, 2018a.

[4] J. Murphy and C. F. Payen, *Oil-to-chemical: New Approach*, PTQ, Brazil, 2020.

[5] I. Amghizar, L. A. Vandewalle, K. M. Van Geem, and G. B. Marin, "New trends in olefin production," *Engineering*, vol. 3, no. 2, pp. 171–178, 2017.

[6] N. Chakinala and A. G. Chakinala, "Process design strategies to produce p-xylene via toluene methylation: a review," *Industrial & Engineering Chemistry Research*, vol. 60, no. 15, pp. 5331–5351, 2021.

[7] A. Corma Canós, L. Sauvanaud, Y. Mathieu, L. Almanza Rubiano, C. Gonzalez Sanchez, and T. Chanaga Quiroz, "Alternative to visbreaking or delayed coking of heavy crude oil through a short contact time, solid transported bed cracking process," *Catalysis Science and Technology*, vol. 8, no. 2, pp. 540–550, 2018.

[8] M. A. B. Siddiqui, A. Aitani, M. R. Saeed, N. Al-Yassir, and S. Al-Khattaf, "Enhancing propylene production from catalytic cracking of Arabian Light VGO over novel zeolites as FCC catalyst additives," *Fuel*, vol. 90, no. 2, pp. 459–466, 2011.

[9] K. Chen, H. Zhang, D. Liu, H. Liu, A. Guo, and Z. Wang, "Investigation of the coking behavior of serial petroleum residues derived from deep-vacuum distillation of Venezuela extra-heavy oil in laboratory scale coking," *Fuel*, vol. 219, pp. 159–165, 2018.

[10] H. Hakimian, S. Valizadeh, Y. M. Kim, and Y. K. Park, "Production of valuable chemicals through the catalytic pyrolysis of harmful oil sludge over metal-loaded HZSM-5 catalysts," *Environmental Research*, vol. 214, Article ID 113911, 2022.

[11] Y. T. Cheng and G. W. Huber, "Chemistry of furan conversion into aromatics and olefins over HZSM-5: a model biomass conversion reaction," *ACS Catalysis*, vol. 1, no. 6, pp. 611–628, 2011.

[12] X. Duan, H. Sun, and S. Wang, "Metal-Free carbocatalysis in advanced oxidation reactions," *Accounts of Chemical Research*, vol. 51, no. 3, pp. 678–687, 2018.

[13] A. Corma and A. V. Orchilles, "Current views on the mechanism of catalytic cracking," *Microporous and Mesoporous Materials*, vol. 35-36, pp. 21–30, 2000.

[14] M. Alabdullah, T. Shoinkhorova, A. Rodriguez-Gomez et al., "Composition-performance relationships in catalysts formulation for the direct conversion of crude oil to chemicals," *ChemCatChem*, vol. 13, no. 7, pp. 1806–1813, 2021.

[15] J. M. Newsam, "The zeolite cage structure," *Science*, vol. 231, no. 4742, pp. 1093–1099, 1986.

[16] S. Suganuma and N. Katada, "Innovation of catalytic technology for upgrading of crude oil in petroleum refinery," *Fuel Processing Technology*, vol. 208, Article ID 106518, 2020.

[17] E. T. C. Vogt and B. M. Weckhuysen, "Fluid catalytic cracking: recent developments on the grand old lady of zeolite catalysis," *Chemical Society Reviews*, vol. 44, no. 20, pp. 7342–7370, 2015.

[18] W. Vermeiren and J. P. Gilson, "Impact of zeolites on the petroleum and petrochemical industry," *Topics in Catalysis*, vol. 52, no. 9, pp. 1131–1161, 2009.

[19] M. Ghashghaee, "Heterogeneous catalysts for gas-phase conversion of ethylene to higher olefins," *Reviews in Chemical Engineering*, vol. 34, no. 5, pp. 595–655, 2018.

[20] M. Ghashghaee and V. Farzaneh, "Nanostructured hydrotalcite supported RuBaK catalyst for direct conversion of ethylene to propylene," *Russian Journal of Applied Chemistry*, vol. 91, no. 6, pp. 972–976, 2018.

[21] R. Ravandi, R. Khoshbin, and R. Karimzadeh, "Synthesis of free template ZSM-5 catalyst from rice husk ash and co-modified with lanthanum and phosphorous for catalytic cracking of naphtha," *Journal of Porous Materials*, vol. 25, no. 2, pp. 451–461, 2018.

[22] R. Khoshbin and R. Karimzadeh, "The beneficial use of ultrasound in free template synthesis of nanostructured ZSM-5 zeolite from rice husk ash used in catalytic cracking of light naphtha: effect of irradiation power," *Advanced Powder Technology*, vol. 28, no. 3, pp. 973–982, 2017.

[23] R. Javaid, K. Urata, Sh. Furukawa, and T. Komatsu, "Factors affecting coke formation on H-ZSM-5 in naphtha cracking," *Applied Catalysis A: General*, vol. 491, pp. 100–105, 2015.

[24] J. Li, X. Li, G. Zhou et al., "Catalytic fast pyrolysis of biomass with mesoporous ZSM-5 zeolites prepared by desilication with NaOH solutions," *Applied Catalysis A: General*, vol. 470, pp. 115–122, 2014.

[25] W. Schwieger, A. G. Machoke, T. Weissenberger et al., "Hierarchy concepts: classification and preparation strategies for zeolite containing materials with hierarchical porosity," *Chemical Society Reviews*, vol. 45, no. 12, pp. 3353–3376, 2016.

[26] M. Caillot, A. Chaumonnot, M. Digne, and J. A. van Bokhoven, "The variety of Brønsted acid sites in amorphous aluminosilicates and zeolites," *Journal of Catalysis*, vol. 316, pp. 47–56, 2014.

[27] M. A. AlAbdullah, A. R. Gomez, J. Vittenet et al., "A viewpoint on the refinery of the future: catalyst and process challenges," *ACS Catalysis*, vol. 10, no. 15, pp. 8131–8140, 2020.

[28] A. Al-Absi, A. M. Aitani, and S. S. Al-Khattaf, "Thermal and catalytic cracking of whole crude oils at high severity," *Journal of Analytical and Applied Pyrolysis*, vol. 145, Article ID 104705, 2019.

[29] M. S. Rana, F. S. AlHumaidan, and R. Navvamani, "Synthesis of large pore carbon-alumina supported catalysts for hydrodemetallization," *Catalysis Today*, vol. 353, pp. 204–212, 2020.

[30] F. Sotomayor, K. Cychosz, and M. Thommes, "Characterization of micro/mesoporous materials by physisorption: concepts and case studies," *Acc. Mater. Surf. Res.*, vol. 3, pp. 34–50, 2018.

[31] J. Wang, L. Abdelouahed, M. Jabbour, and B. Taouk, "Catalytic hydro-deoxygenation of acetic acid, 4-ethylguaiacol, and furfural from bio-oil over Ni 2 P/HZSM-5 catalysts," *Comptes Rendus Chimie*, vol. 24, no. S1, pp. 131–147, 2021.

[32] D. García-Pérez, M. C. Alvarez-Galvan, J. M. Campos-Martin, and J. L. G. Fierro, "Influence of the reduction temperature and the nature of the support on the performance of zirconia and alumina-supported Pt catalysts for n-dodecane hydroisomerization," *Catalysts*, vol. 11, no. 1, 2021.

[33] H. G. Karge, "Characterization by IR spectroscopy," *Verified Syntheses of Zeolitic Materials*, International Zeolite Association, 2nd Ed edition, 2002.